# Lithospheric stresses caused by mantle convection: the role of plate rheology

Thorsten W. Becker and Richard J. O'Connell
Department of Earth and Planetary Sciences, Harvard University, Cambridge MA, USA (becker@geophysics.harvard.edu)

Fall AGU 2001

## Abstract

We model deformation and stress in the lithosphere using a combination of a global circulation model for the mantle and a finite element approximation (SHELLS) for the lithosphere. We confirm that mantle flow can explain the large scale stress field when past subduction or tomography is interpreted as density driving the plates. A more realistic treatment of the lithosphere with non-Newtonian creep and faults with Byerlee friction does not improve the fit to observed stress orientations, but leads to different amplitude predictions and modifies the crustal stress regime pattern. Further work on similar models should lead to a more complete understanding of mantle-lithosphere interactions, important to study the formation of plate boundaries and seismic hazard.

## Introduction

To understand the effect of mantle flow on deformation and stress in the lithosphere it is necessary to model both convection in the mantle and brittle-ductile flow in the plates. Especially the advance of better constrained mantle density models has made recent attempts of using global flow models of the Hager & O'Connell (1981) type to predict stresses in the lithosphere (Steinberger et al., 2001) more successful than earlier work by Bai et al. (1992). While those kinds of models used a homogeneous shell approximation, Bird (1998) presented a finite element model of the lithosphere as a shell with faults, Byerlee type brittle deformation and non-Newtonian creep laws. Bird included considerable crustal complexity but simplified driving flow patterns at the base of the plates.

Here, we will use SHELLS, Peter Bird's program (Kong and Bird, 1995), and global flow models based on tomography and Cenozoic subduction to study the effect of the rheology of the lithosphere. We start from simplified models and introduce complications step by step to explore the complexity that is needed to explain observations such as the World Stress and Strain Maps and the distribution of seismic moment release.

## Observations

### Seismicity

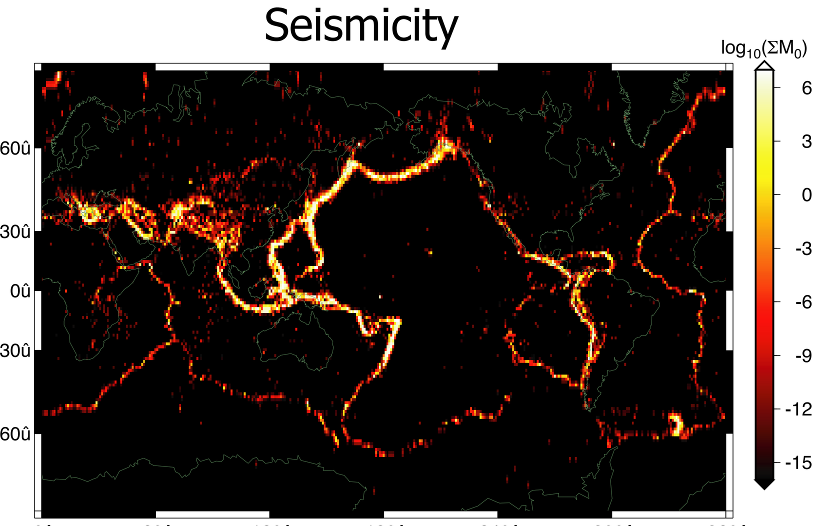

We show the decadic log of cumulative moment release of all seismicity shallower than 80 km from the Engdahl et al. (1998) catalog in 1 degree bins. Note the varying strength of seismicity along plate boundaries and intraplate deformation belts.

### World Strain Rate Map

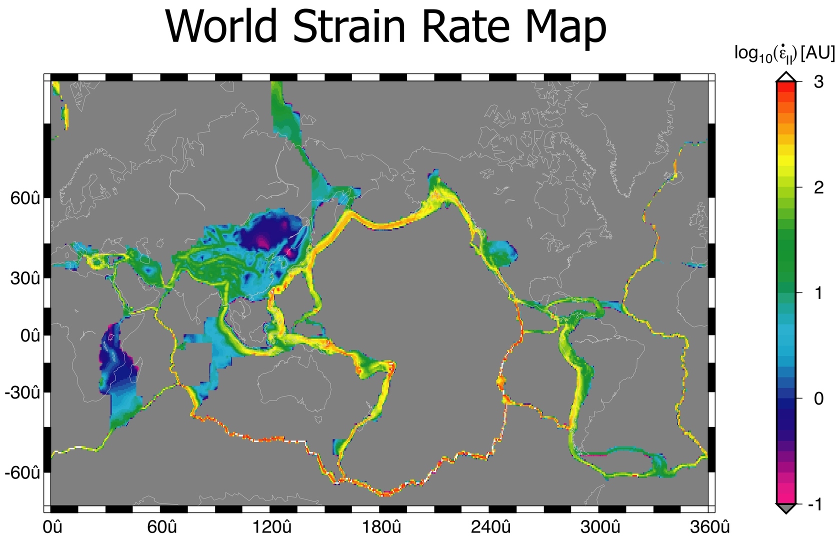

The UNAVCO World Strain Rate Map (Holt et al., 2000) is based on CMT solutions, fault slip rates and geodetic surveys. While we show a scalar quantity (second invariant of strain rate, compare to cumulative moment), tensorial information should eventually become more useful than WSM data to constrain models.

### World Stress Map

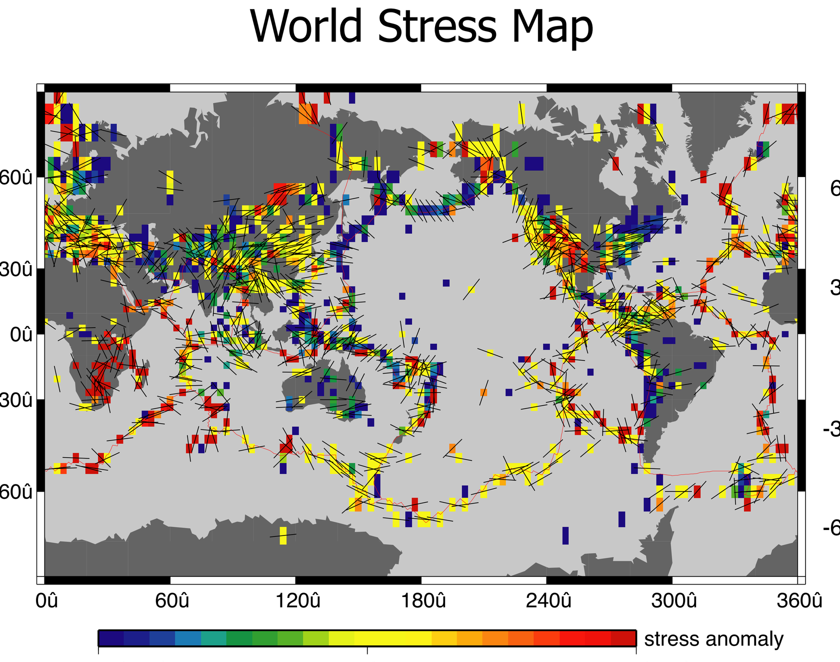


We show 5 degree binned quality C or better data from the World Stress Map (WSM, Mueller et al., 2000) based on focal mechanisms, hydro frac and overcoring measurements. Colors indicate inferred stress regime and sticks denote compressional stress direction. Data is very non-uniform and affected by local phenomena.

### Bird stress interpolation

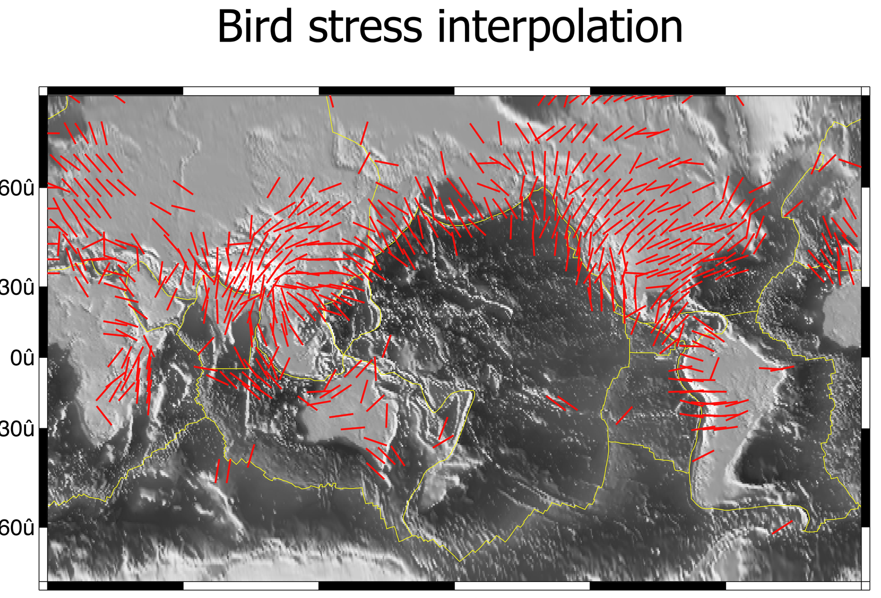

Bird and Li (1996) published an interpolation of WSM (compressional stress axis only) data based on an earlier release of the data base. When used for scoring models, this interpolation is biased by North America, East Asia, and Europe where stress directions are well constrained. We will therefore also use our compilation (left), keeping the problems of the raw WSM data in mind.

Indicators of the direction of regional stress are of varying quality, and we will see that the well constrained large scale features can be reproduced by a number of models. Geodetic and seismic strain observations will therefore be needed to distinguish more clearly between models, and only those can be expected to yield better control on the magnitude of the tensor components.

## Method

For the mantle part, we use a Hager & O'Connell (1981) calculation which solves Stokes flow for only radially varying viscosity given a density field and velocity or stress boundary conditions. We compute the sub-lithospheric velocities to use them as a boundary condition on the base of the lithospheric model, either from density driven flow with a free surface or plate driven flow with a no-slip constraint. Previous work and our studies on the comparison between tomographic and geodynamic models (Becker & Boschi, submitted) and plate driving force inversions (Becker & O'Connell, submitted) guides us as to the choice of parameters. A best-fit radial viscosity profile from Mitrovica and Forte (1997) with a stiffer lithosphere ($10^{22}$ Pas) is used throughout (for sensitivity of stress kernels to viscosity see Steinberger et al., 2001).

We use the 2.5-D spherical finite element code SHELLS (solution of vertically averaged equilibrium equations; Kong & Bird, 1997) to increase the realism of previous models with respect to the treatment of plate rheology. However, we simplify the model with respect to Bird (1998): material parameters are (in a first step) not allowed to vary with depth and a homogeneous shell thickness of 100 km is used. The simplest lithosphere obeys a Newtonian creep law; enhancements include pure power-law flow with power law exponent n=3.5 and faults that incorporate velocity discontinuities with a Byerlee law for the maximum brittle shear stress. The viscosity of the finite element model is chosen such that its average is equal to the viscosity of the lithosphere of the circulation model it replaces. We have verified that the stress field predictions using SHELLS are similar to those of global flow calculations for the test case of a purely Newtonian lithosphere.

The finite element mesh on which the continuum equations are solved is subject to several constraints: quality bounds on deformed elements, inclusion of realistic plate boundaries, optional mesh refinement, and equal area elements else. Our approach to the gridding problem uses an automated script that constructs and then combines individual plates based on the NUVEL-1 plate boundaries (DeMets et al., 1990) using the TRIANGLE Delaunay mesher (Shewshuk, 1996). Plate boundary types are detected as in Becker & O'Connell (submitted) and we assign fault dip angles depending on the inferred plate boundary types as in Bird (1998).

A

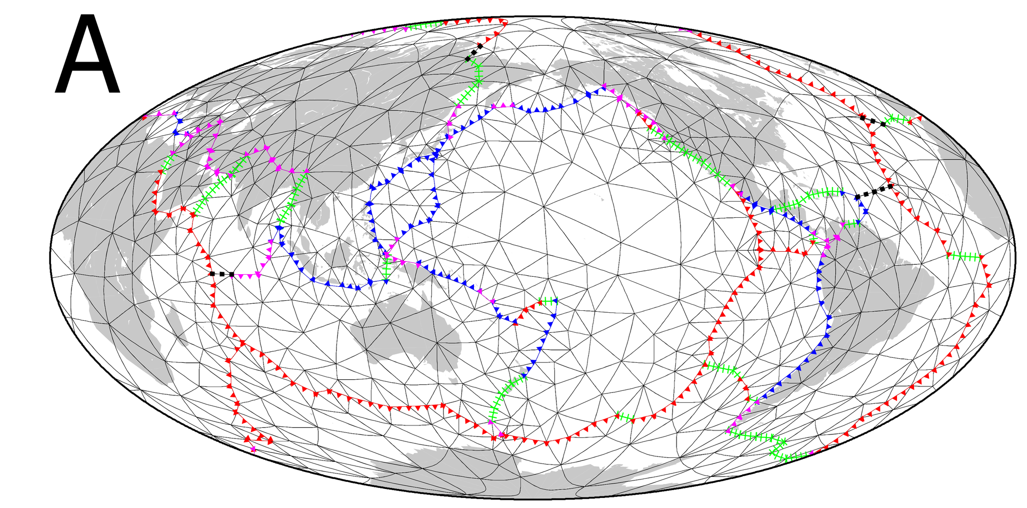

Blue: convergent margin, dipping 25 degree, magenta: convergent, dipping 32 degree, red: divergent, dipping 60 degree, green: transform, dipping 90 degree from the horizontal.

B

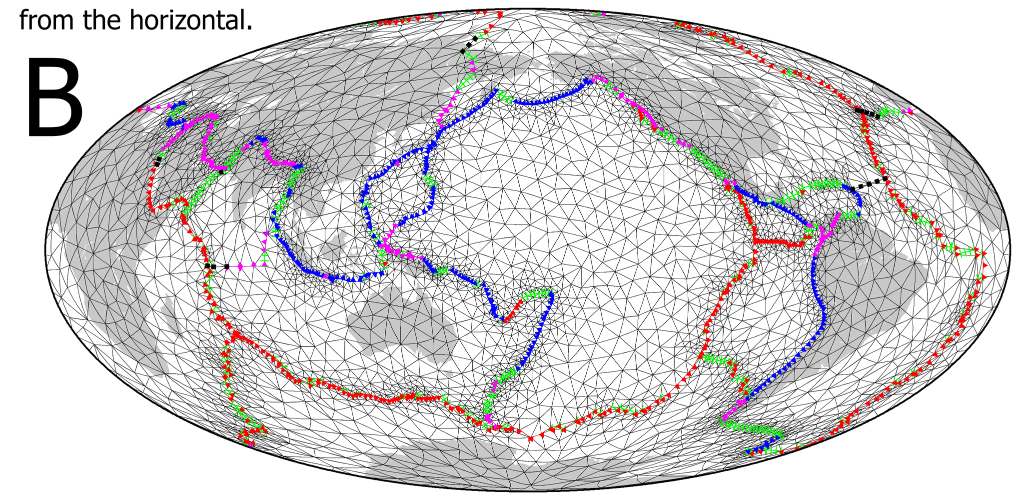

## Results

### Stress predictions for a Newtonian lithosphere

Lithospheric stress results from effects such as potential energy differences in the crust and mantle flow; we isolate different contributions for simplicity. Below, we show the compressional stress axis (with fixed scale), length is proportional to the maximum shear stress. Mean normal stress is color coded in the background (red=extension, blue=compression). We also include hotspots from Steinberger (2000) with sizes scaled to inferred mass flux.

S20RTS driven plates

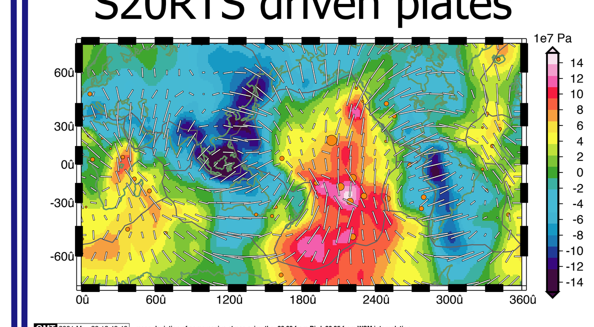

SB4L18 driven plates

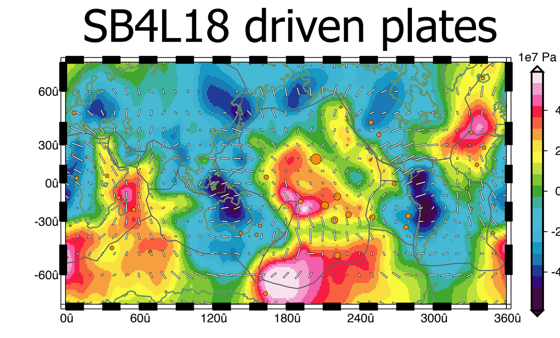

nGRAND driven plates

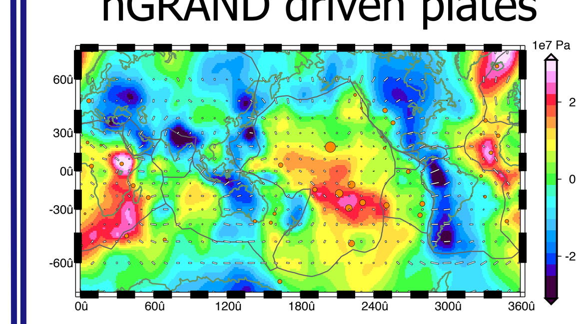

STEIN driven plates

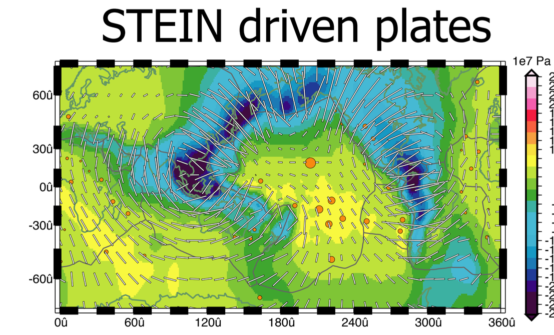

Litho. thickening driven

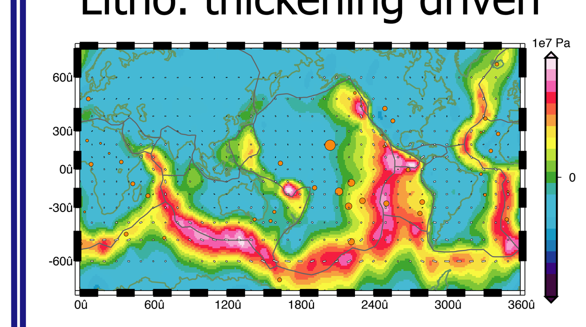

NUVEL-1 plate motions

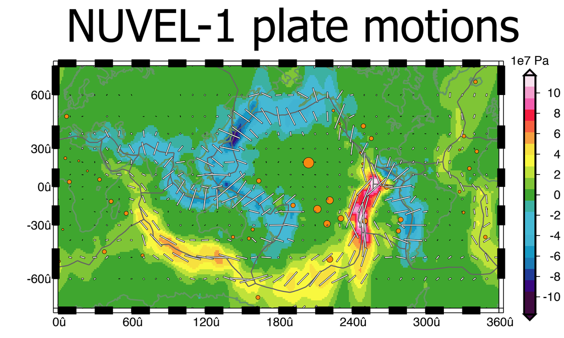


Results are consistent with Steinberger et al. (2001): mantle driven models yield good fits to the observed stress field in general but vary in the details. We find that S20RTS achieves a better score than any model of Bird (1998). The main effect of mantle flow is related to subduction, leading to compression around the Pacific. Upwellings underneath Africa and the central Pacific lead to extension in those areas, not found in ridge-push type models.

mean deviations of comp axis

| | Bird&Li [deg] | WSM [deg] |
|---|---|---|
| lith thick | 39 | 42 |
| NUVEL | 36 | 42 |
| SB4L18 | 34 | 40 |
| nGRAND | 33 | 39 |
| STEIN | 32 | 41 |
| S20RTS | 29 | 36 |

## Effect of rheology

We show predictions of horizontal stress for flow driven by the best fitting tomography model, S20RTS, and vary the rheology of the lithosphere (mesh A). The friction coefficient for faults is chosen such that max shear stresses are ~1 MPa (weak faults).

Newtonian creep

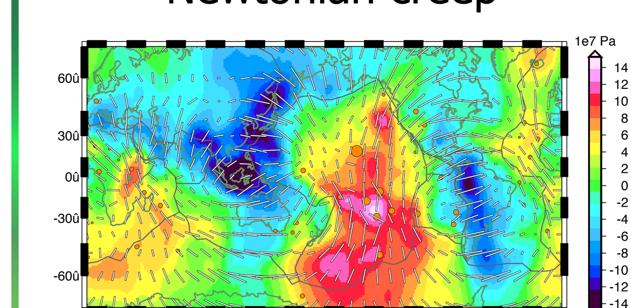

power-law creep

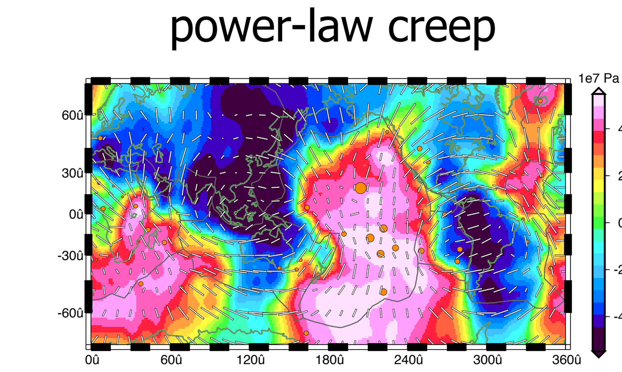

Newtonian creep & weak faults

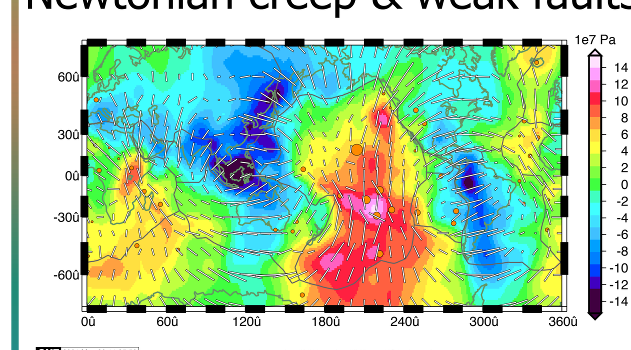

power-law creep & weak faults

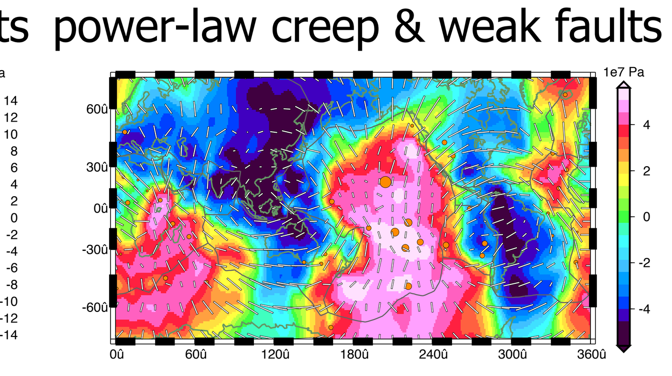

We find that the large scale orientation of the principal stresses is not strongly affected by the lithospheric rheology, and the fit to observations stays roughly the same. The tendency of the power law rheology to reduce stress localization leads, however, to changes in the tectonic stress amplitudes and patterns, especially for the maximum shear stress. Faults in Newtonian flow appear to have only a minor effect on a regional scale but can lead to segmentation along margins in combination with power-law creep. This effect is strong for plate-like motion (see Figure below for power-law & faults for NUVEL-1) and will be explored further in more detailed models.

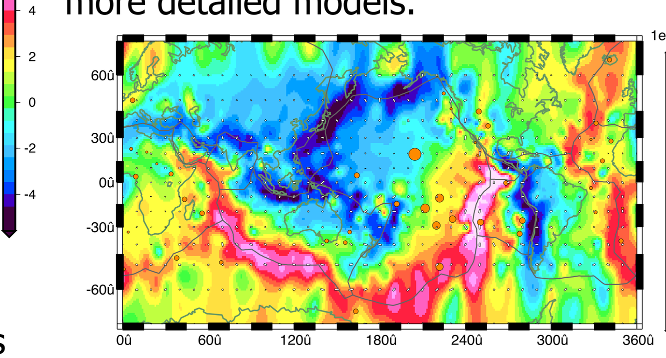

In the same fashion as above, we show predictions of the max shear stress fields for different rheologies. Black contours denote observed seismicity.

Newtonian creep

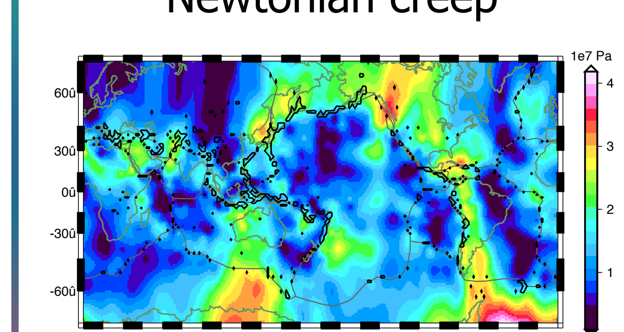

power-law creep

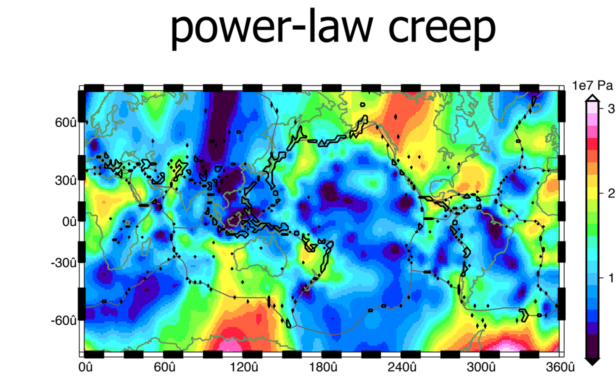

Newtonian creep & weak faults

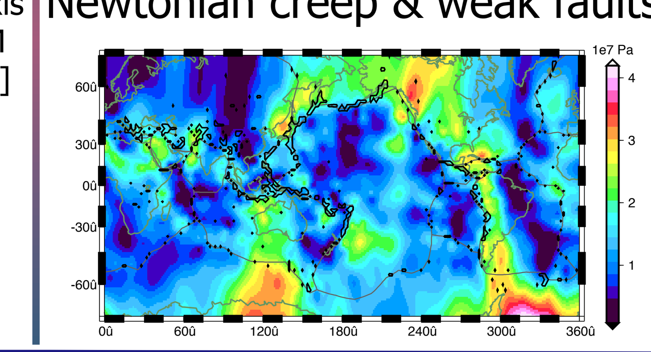

power-law creep & weak faults

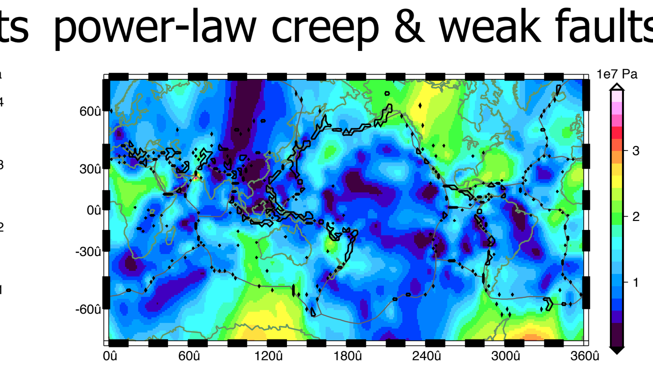

### Resolution test

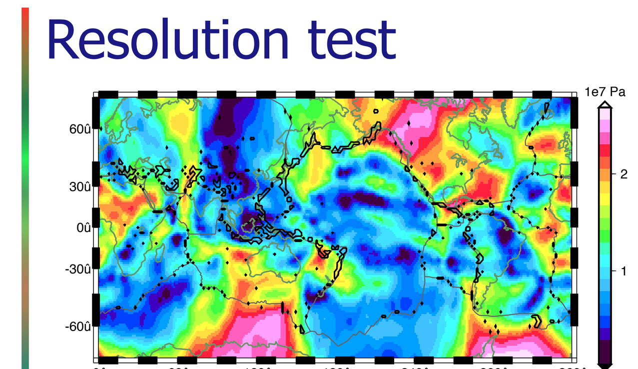

The Figure above shows a mesh B calculation of the shear stress for power-law creep to be compared with its left neighbor which was based on mesh A. Results are consistent but especially the treatment of faults will probably require a higher mesh

## Conclusions

We confirm that mantle flow is a valid mechanism for explaining the observed plate stresses; convective drag forces should be explicitly included in models of lithospheric deformation. Stress field orientations are stable with respect to lithospheric rheology. However, the sensitivity of the maximum shear stress shows that the inclusion of surface complexity might be required to arrive at better fits of observed strain rates and seismicity, needed to put inferences on plate boundary dynamics and seismic hazard on firmer ground.

## Acknowledgements

We thank Peter Bird for making his finite element code available, Bernhard Steinberger for providing the original global circulation program, and all authors of the tomography and geodynamic models for sharing their results. All Figures were produced with GMT by Wessel and Smith (1992).